ELSEVIER

Journal of Hydrology 256 (2002) 60–79

Journal of Hydrology

www.elsevier.com/locate/jhydrol

Liquid-release tests in unsaturated fractured welded tuffs: I. Field investigations

Rohit Salve*, Joseph S.Y. Wang, Christine Doughty

E.O. Lawrence Berkeley National Laboratory, Earth Sciences Division, University of California, #1 Cyclotron Road, MS 14-116, Berkeley, CA 94720, USA

Received 21 February 2001; revised 9 July 2001; accepted 5 September 2001

Abstract

Wetting-front movement, flow-field evolution, and drainage of fracture flow paths were evaluated within the Topopah Spring welded tuff at Yucca Mountain, Nevada. Equipment and techniques were developed for in situ quantification of formation intake rates, flow velocities, seepage rates, and volumes of fracture flow paths. Localized injections of liquid into a low-permeability zone (LPZ) and a high-permeability zone (HPZ) along a borehole were detected in two boreholes below the point of injection. For the LPZ tests, water did not seep into an excavated slot that defined the lower boundary of the test bed, and the liquid-intake rate under constant-head conditions was observed to steadily decrease by two orders of magnitude. In the HPZ, liquid-intake rates under constant-head conditions were significantly higher and did not exhibit a strong systematic decline. HPZ tests were also conducted under a range of constant-flow conditions. Slot seepage rates showed intermittent responses and the percentage of injected water recovered in the slot increased as each test progressed. A maximum of 80% of the injected water was recovered during high-rate injection tests. The flow path volumes were found to increase during the course of each HPZ test. The data collected during these field tests has provided useful information for developing an understanding of liquid flow in unsaturated fractured welded tuff. It has also provided a basis for quantitative comparisons with numerical simulations of liquid-release experiments, as demonstrated in a companion paper [J. Hydrol. 256 (2002)].

Keywords: Vadose zone; Welded tuff; Fractures; Seepage

1. Introduction

A clear understanding of flow and transport in the unsaturated, fractured rock environment is essential for the development of Yucca Mountain as a potential geological repository of spent fuels and high-level nuclear waste, as well as for efficiently remediating contaminated sites and effectively designing and monitoring hazardous waste storage facilities situated in unsaturated fractured rock elsewhere. Recent observations related to flow of liquids at Yucca Mountain indicate that fractures can be primary flow paths in the unsaturated zone. A model that incorporates fracture-dominated flow conditions would be a strong departure from early conceptual models of matrix-dominated flow, which (based on capillary considerations) envisioned flow to occur primarily through the rock matrix under ambient unsaturated conditions

* Corresponding author. Fax: +1-510-486-6608.
E-mail addresses: r_salve@lbl.gov (R. Salve), jswang@lbl.gov (J.S.Y. Wang), cadoughty@lbl.gov (C. Doughty).

0022-1694/02/$ - see front matter
PII: S0022-1694(01)00519-4

Table 1
Range of scales for studying flow and transport in unsaturated fractured rock

Type of experiment	Scale (m)	Features						Example
		Fracture heterogeneity	Matrix considered	Visualize processes	Monitoring coverage	Controlled source	Realistic background conditions	
Laboratory-glass plates	0.1–0.3	Known, artificial	No	Yes	Good	Yes	No	Lenormand and Zarcone, 1989
Laboratory-transparent fracture replica	0.1–0.3	Known, real	No	Yes	Good	Yes	No	Persoff and Pruess, 1995
Laboratory-block of fractured rock	0.1–1	Partially known	Yes	No	Good	Yes	No	Haldeman et al., 1991
Field site-special access	1–10	Partially known	Yes	No	Good	Yes	Yes	Present study
Field site-surface and borehole access	10–100	Unknown	Yes	No	Sparse	Yes	Yes	Faybishenko et al., 2000
Field site-borehole access	100–1000	Unknown	Yes	No	Sparse	No	Yes	Davidson et al., 1998
Field site-surface access	Unknown	Unknown	Yes	No	None	Yes	Yes	Kilbury et al., 1986

(Montazer and Wilson, 1984; Wang and Narasimhan, 1985). Such a shift in paradigm would have significant ramifications on repository design and performance (e.g. Doughty and Pruess, 1992).

Evidence for fracture-dominated flow is largely based on indirect field observations, including the presence of perched water bodies with apparent ages younger than water in the surrounding tuff matrix (Pruess et al., 1999), water-associated mineral deposits on fracture surfaces (Paces et al., 1996), and bomb-pulse ^{36}Cl signals detected at isolated locations within the mountain (Fabryka-Martin et al., 1996). Direct evidence of flow in fractures remains elusive, largely because of technical difficulties encountered in locating and measuring fracture flow underground.

Early conceptual models developed to describe flow through unsaturated fractures, with fractures and matrix explicitly taken into account (e.g. Wang and Narasimhan, 1985; Pruess and Wang, 1987; Pruess and Tsang, 1990; Nitao and Buscheck, 1991), are based on the underlying premise of capillary equilibrium between fractures and matrix. Because capillary forces are much stronger in the matrix, mobile liquid will not exist anywhere in the fracture unless the surrounding matrix is nearly fully saturated, in which case the fracture will be locally saturated as well. Hence, unsaturated flow along the fracture plane depends strongly on the continuity of locally saturated aperture segments. Pruess (1999) argues for a rather different scenario, with water flowing freely in networks of interconnected fractures while the surrounding matrix remains unsaturated. Another alternative view presented by Tokunaga and Wan (1997) suggests that significant water flux could occur as film flow in unsaturated fractures, with heterogeneities in both the fracture aperture distribution and the surface roughness controlling the fluid flow-field. The wide divergence of the above models emphasizes the necessity of exploring fracture flow and fracture/matrix interactions in situ.

This paper presents the results of a field investigation on fracture flow and fracture/matrix interactions in the Topopah Spring welded tuff rocks (TSw) at Yucca Mountain, using techniques developed specifically for in situ testing of flow in fractured rock at the scale of 1–3 m. Numerical modeling studies done in conjunction with the field tests are presented in a companion paper (Doughty et al., 2001). The objective of this study was to estimate hydraulic parameters such as formation intake rates (the rates at which water flows into the fractured rock from a ponded surface), flow velocities (inferred from the time taken for the wetting-front to travel a known distance within the formation), seepage rates (the volumetric flow rates out of the formation into an underlying excavation), and flow-path volumes under controlled boundary conditions. Field tests were designed to study the evolution of focused flow arising from localized liquid-releases, because the release of contaminated fluid is likely to be localized either after waste-package failure or from transient high infiltration events. Under these conditions, the most practical procedure is to observe fracture flow, and then try to infer fracture/matrix interactions. Direct observation of fracture/matrix interactions can be done by using dyed liquid and mining back the rock after a liquid-release test, but this precludes repeating experiments under a range of initial and boundary conditions.

Table 1 summarizes a range of spatial scales at which investigations of flow and transport in unsaturated fractured rocks may be conducted. Generally, as scale increases, the ability to incorporate more realism into an experiment grows, but the ability to monitor processes decreases. Because of the complexity of the natural system, it is difficult to know how to apply results obtained at a given scale to larger or smaller scales. Thus, it is valuable to study behavior at a variety of scales, both to provide the basis for developing practical means of upscaling, and to examine the distinctive responses of the various scales. The 1–3 m scale considered in the present study is the characteristic dimension of the individual waste packages for the proposed Yucca Mountain repository.

Several other research groups are also using in situ liquid-release experiments to investigate the interplay of fracture flow and fracture/matrix interactions in unsaturated rock at the scale of a few meters. Each experiment incorporates a special feature that enables more extensive monitoring than would ordinarily be available using boreholes alone. At several sites in the ESF at Yucca Mountain, slugs of dyed water were released into boreholes overlying excavated niches and dye patterns were photographed on the niche ceilings (Wang et al., 1999). At Hell's Half

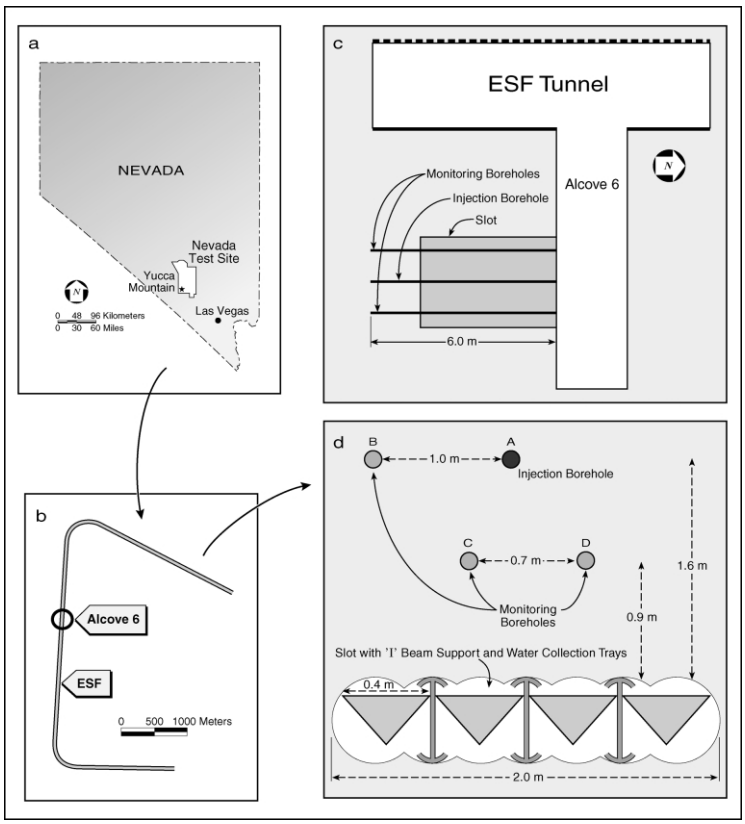

Fig. 1. (a) and (b) Plan view of location and (c) vertical view of layout (d) of test bed within the ESF at Yucca Mountain. Figures (c) and (d) are not drawn to scale.

Acre in the Snake River Plain, Idaho, a ponded infiltration test was conducted on an overhanging basalt rock containing two prominent fractures; water arrivals (drips) on the underside of the rock were mapped and counted (Podgorney et al., 2000). In the Negev desert in Israel, traced water was ponded on a horizontal bench of a chalk cliff face where a vertical fracture was exposed. An underlying horizontal borehole intersected the vertical fracture to provide access for monitoring moisture and tracer arrivals (Dahan et al., 1998, 1999). Unfortunately, in all these experiments some of the introduced water was able to bypass the monitoring system, making quantitative mass balances comparing fracture flow and matrix imbibition impossible.

2. Methods

Field experiments were conducted in fractured, welded tuff within Yucca Mountain over a period of six weeks starting in late July 1998 (Fig. 1a). These experiments included multiple releases of tracer-laced water in one low-permeability zone (LPZ) and one high-permeability zone (HPZ) along a horizontal injection borehole. Permeabilities of these zones were determined from air-permeability measurements conducted over 0.3 m sections along the borehole (Cook, 2000). The measured air-permeability was 2.7×10^{-13} and 6.7×10^{-12} m^2 for the LPZ and HPZ, respectively. During and following liquid-release events, changes in saturation and water potential in the fractured rock were measured in three monitoring boreholes. These changes were continuously recorded by an automated data acquisition system. Water that seeped into the excavated slot below the injection zone was collected, quantified for volumes and rates, and analyzed for tracers.

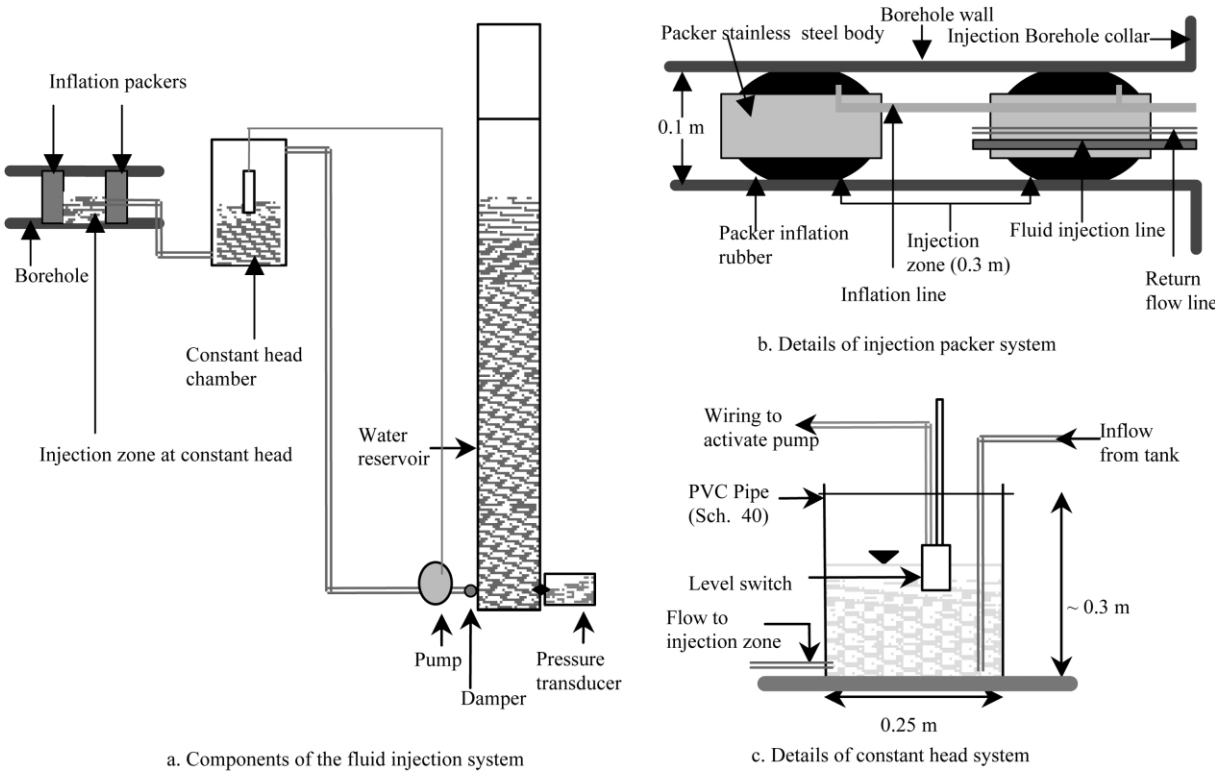

Fig. 2. Liquid-release system for constant-head and constant-rate injections.

2.1. The test bed

The test bed is located approximately ~210 m below the surface of the mountain in an Alcove (Alcove 6) in the Exploratory Studies Facility (ESF, see Fig. 1b and c), within the middle nonlithophysal portion of the TSw. The rock is visibly fractured with predominantly vertical fractures and few subhorizontal fractures. Relatively wide fracture spacing (on the order of tens of centimeters) facilitated the choice of injection zones, allowing discrete fractures and well-characterized fracture networks to be isolated by packers for localized flow testing.

A horizontal slot and a series of horizontal boreholes are the distinct features of the test bed (Fig. 1d). The slot, located below the test bed, was excavated by an over-coring method. The excavation sequence required first the drilling of parallel pilot holes, 0.10 m in diameter, over 4 m in length, with a 0.22 m spacing, normal to the alcove wall. The pilot holes were then over-cored by a 0.3 m drill-bit to excavate the 2.0 m wide, 4.0 m deep and 0.3 m high slot located approximately 0.8 m above the alcove floor. Three I-beam supports were installed along the length of the slot for support. Four horizontal boreholes, 0.1 m in diameter and 6.0 m in length, were drilled perpendicular to the alcove wall above the slot. Boreholes A and B were located 1.6 m above the slot ceiling, while boreholes C and D were 0.9 and 1.0 m above the slot ceiling, respectively, and 0.7 m apart (Fig. 1d).

Borehole A was used for fluid injection while boreholes B, C and D were monitored for changes in moisture conditions. The slot was used to collect water seeping from the fractured rocks above. A flexible plastic curtain 3.0 m wide and 0.9 m high was installed to cover the slot face and minimize air movement between the alcove and slot.

2.2. Instrumentation

There were three distinct components to the flow

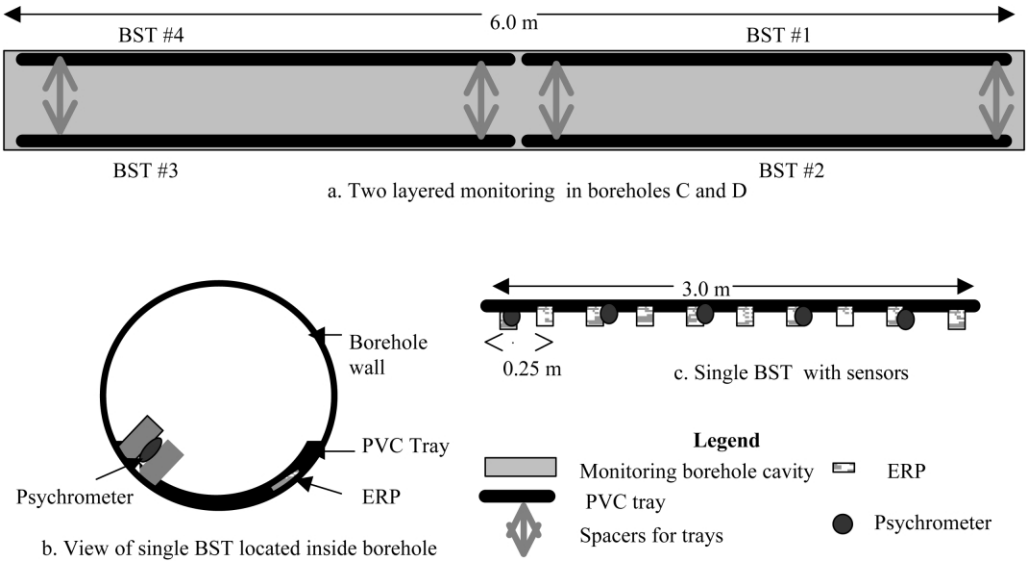

Fig. 3. Borehole monitoring system.

investigation: (1) controlled release of water into isolated zones, (2) borehole monitoring for changes in saturation and water potential, and (3) collection of seepage from the slot ceiling. Key features of new instruments developed for this field investigation are described later.

2.2.1. Fluid injection

The liquid-release experiments required water to be injected into the formation over a 0.3 m zone in the borehole under constant-head or constant-rate conditions. The constant-head tests were conducted first to determine the maximum rates at which the zone could take in water. The subsequent set of experiments required that water be released to the formation at predetermined rates ranging from ~5 to ~100 ml/min. Both the constant-head method and the constant-rate method of injection were incorporated in the fluid-release apparatus. The main components of the fluid release apparatus included an inflatable packer system for isolating the injection zone, a pump for delivering water, and a reservoir for providing a continuous supply of water (Fig. 2a).

The inflation packer system consisted of two rubber packers, each 0.60 m long, connected to an inflation line (Fig. 2b). Two stainless tubes (0.95 and 0.31 cm ID) passed through one of the packers to provide fluid (air and water) access into the injection zone. The 0.95 cm tube was used to deliver fluid into the injection zone, while the 0.31 cm tube was used as a siphon to remove excess water from the injection zone. Before liquid was released into the formation, the packer system was located to straddle the zone of interest (determined from air-permeability measurements) and then inflated to a pressure of ~200 kPa. The 0.95 cm ID stainless steel tube was then connected to a water supply line from a constant-head or a constant-rate system. During the entire period of injection, pressure in the inflation packers was continuously monitored to ensure that the injection zone remained isolated from adjacent zones of the borehole.

To capture the temporal variability in the vertical flux of water from the injection zone, an automated liquid-release system was developed. This system allowed for continuous measurement of local liquid-release rates. The unit consisted of a water reservoir (~4.5 l) for water supply to a clear acrylic constant-head chamber. The chamber, 0.25 m ID and 0.30 m tall, served to maintain a constant-head of water above the liquid-release surface within the injection zone (Fig. 2c). The hydraulic head was maintained with a level switch that activated the pump when the water level dropped below the control level. The control

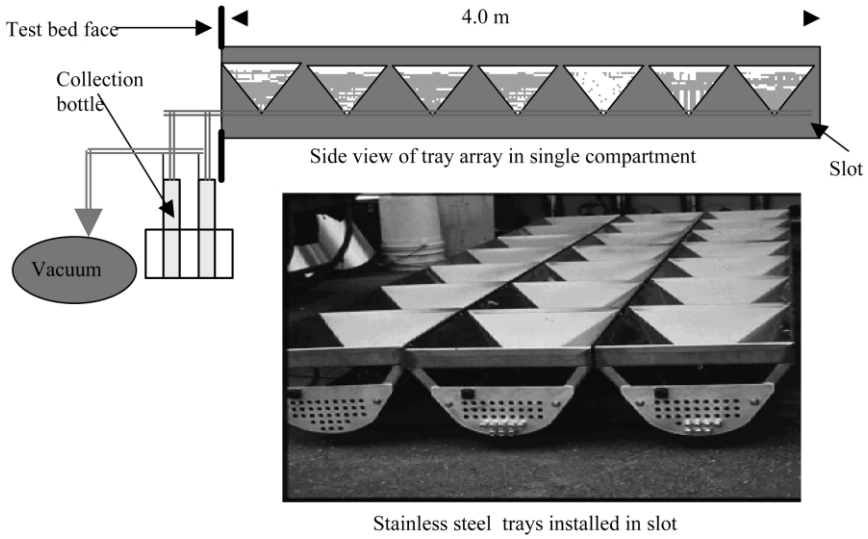

Fig. 4. Water-collection system installed in slot.

level was nominally set at or slightly above the elevation of the horizontal injection borehole. Two pressure transducers located at the base of the reservoir continuously recorded the height of water. A pulse damper was installed between the pump and tank to reduce any pulsating effects (caused by the pump) from migrating to the storage tank and influencing the pressure readings.

The constant-rate injection system included all the components used in the constant-head system without the constant-head chamber. To allow for easy regulation of flow rates in the field, we calibrated the pump before field deployment to relate flow rates with displayed numbers on a 10-turn speed control. In the field, the speed control was set at the desired flow rate before the pump was activated. The actual flow rate was determined from transducers located at the base of the water reservoir. A data acquisition system was used to record changes in head of water in the reservoir.

2.2.2. Borehole monitoring

In three monitoring boreholes (B, C and D in Fig. 1d), relative changes in saturation and water potential were measured continuously during the entire field investigation. Changes in resistance were measured with electrical resistivity probes (ERPs) (Salve et al., 2000). Water potential measurements were made with psychrometers. Using the multiplexing capabilities of the data logger (model CR7, Campbell Scientific Inc.), hourly measurements of up to 80 psychrometers (model PST-55, Wescor Inc.) were automated. The chromel-constantan junction in the psychrometer was cooled with an electric current to a temperature below dew point to induce condensation, followed by evaporation without electric current. The temperature depression resulting from evaporation was recorded and used to determine water potentials in the vicinity of the psychrometers.

The psychrometers and ERPs were housed in borehole sensor trays (BSTs) installed along the length of each monitoring borehole (Fig. 3a). On each tray, psychrometers were installed at 0.5 m intervals along the borehole while ERPs were located at 0.25 m intervals (Fig. 3b and c) The BSTs permitted direct contact between ERPs and the borehole wall. The psychrometers were installed inside small cavities (0.005 m in diameter) perforated through the BST wall to measure water potentials of the rock. A steel spoon, 3.0 m long with the same configuration as the trays, was used to guide each BST to the assigned location along the borehole. Two BSTs were located along each section of borehole, one in contact with the top of the borehole and the other with the bottom. Each pair of BSTs was separated by a wedge,

Table 2
Amount of water and types of tracers released into the injected borehole (LPZ located 0.75–1.05 m from borehole collar; HPZ located 2.30–2.60 m from borehole collar)

Date	Test[a]	Injection type	Infiltration rate (ml/min)	Volume of water injected	Additional tracer[b]
					Sodium bromide
7/23/98	LPZ-1	Constant rate	~16	5.6	2,3,6 Trifluorobenzoic acid
7/23–24/98	LPZ-1	Falling-head			
7/24/98	LPZ-2	Constant-head	~1.2	0.3	2,4,5 Trifluorobenzoic acid
7/24–25/98	LPZ-2	Falling-head		1.2	2,4,5 Trifluorobenzoic acid
7/29–30/98	LPZ-3	Constant-head	~0.5	0.4	3,5 Difluorobenzoic acid
7/30–31/98	LPZ-3	Constant-head	~0.5	0.6	3,5 Difluorobenzoic acid
7/31–8/4/98	LPZ-3	Falling-head		1.2	3,5 Difluorobenzoic acid
8/4/98 10:23	HPZ-1	Constant-head	~119	16.3	Potassium fluoride Pentafluorobenzoic acid
8/4/98 17:11	HPZ-2	Constant-head	~98	17.3	2,3,4 Trifluorobenzoic acid
8/5/98 9:55	HPZ-3	Constant rate	~53	17.5	3,4 Difluorobenzoic acid
8/6/98 9:08	HPZ-4	Constant rate	~5	3.4	2,3,4,5 Tetrafluorobenzoic acid
8/25/98 8:54	HPZ-5	Constant rate	~69	18.4	
8/26/98 8:25	HPZ-6	Constant rate	~38	18.4	
8/27/98 8:36	HPZ-7	Constant rate	~29	18.2	
8/28/98 8:25	HPZ-8	Constant rate	~14	9.4	

[a] Average infiltration rate during release period.
[b] All injected water was tagged with lithium bromide.

which pressed the BSTs tight against the borehole wall.

2.2.3. Seepage collection

To measure water seeping into the slot following liquid-release into the injection borehole, we designed a water collection system to capture seepage from the slot ceiling (Fig. 4). Design of this system was dictated by the slot geometry and locations of 'I' beam supports. A row of stainless steel trays was fabricated for each of the four accessible compartments between the I-beams. Each tray was an inverted pyramid 0.46 m long and 0.40 m wide and tapered to a single point 0.20 m from the top. For each compartment, seven trays were assembled along a single steel frame, allowing for easy installation inside the slot. A total of 28 collection trays were used during the tests. Water captured in the stainless steel trays was transferred into clear PVC collection bottles (0.076 m ID, 0.45 m tall). Water falling onto the trays was drained to the collection bottles through Teflon tubes (0.635 cm OD). An intermittent vacuum was applied to the collection bottles such that water stored on the trays or in Teflon tubes could be sucked into the collection bottles.

2.3. Liquid-release experiments

Air-permeability measurements were conducted along 0.3 m sections of the injection borehole (Cook, 2000). The most and least permeable intervals were identified as the LPZ (0.75–1.05 m from the collar) and the HPZ (2.3–2.6 m from the collar). In both the LPZ and the HPZ, a series of constant-head tests was conducted to determine the temporal changes in the rate at which the formation could take in water. In the HPZ, a second series of tests was conducted with different prescribed injection rates. Tests conducted in this field investigation are summarized in Table 2. The seepage rates into the slot were monitored during all tests.

All water used in the ESF is spiked with lithium bromide for tunnel mining-related activities and for most of the scientific investigations. Additional tracers were added to the water injected into the LPZ and during the first set of experiments in the HPZ (Table 2). During the tests, water that seeped into the slot was periodically sampled and analyzed for tracer concentrations.

Water was released into the LPZ three times over a period of two weeks, starting on 7/23/98 (Table 2).

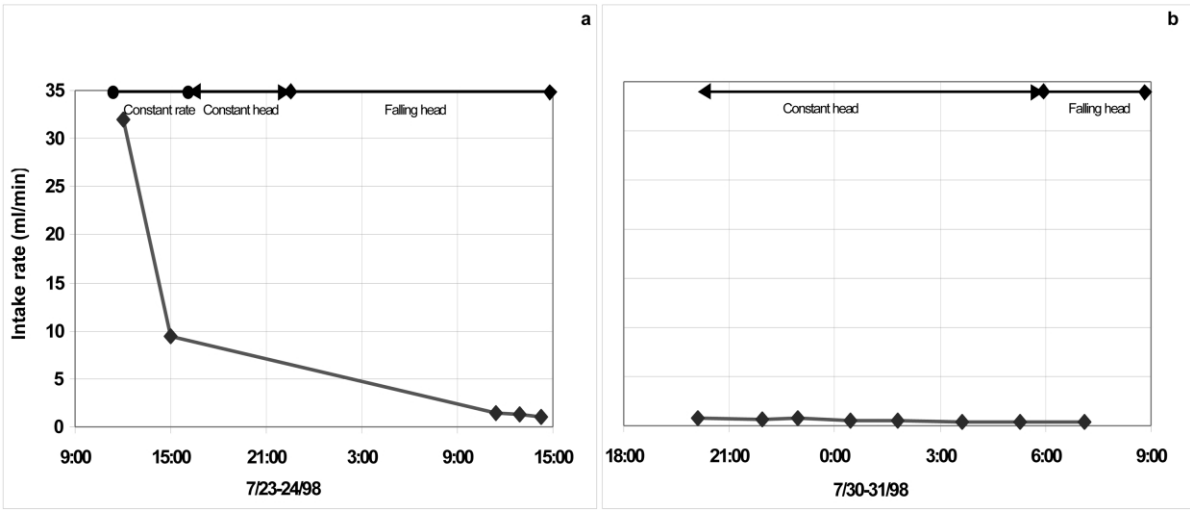

Fig. 5. Water intake rates observed in the LPZ.

For the first event, water was injected at a constant-flow rate of ~56 ml/min. At 66 min, water was observed in the overflow line, indicating that water was being injected at a rate higher than the intake capacity of the zone. At this time, the flow rate on the pump was immediately reduced to ~6.0 ml/min. Within 22 min return flow ceased, and water was injected continuously at this rate for the next 4 h and 23 min. During this injection, a total of 6.3 l of water was injected into the zone of which 0.7 l was recovered as return flow. The other 5.6 l was released into the formation. The average net intake rate into the formation rate was 16 ml/min.

For the second liquid-release in the LPZ, the constant-head injection system was used. The constant-head chamber was located adjacent to the injection borehole such that the head of water was

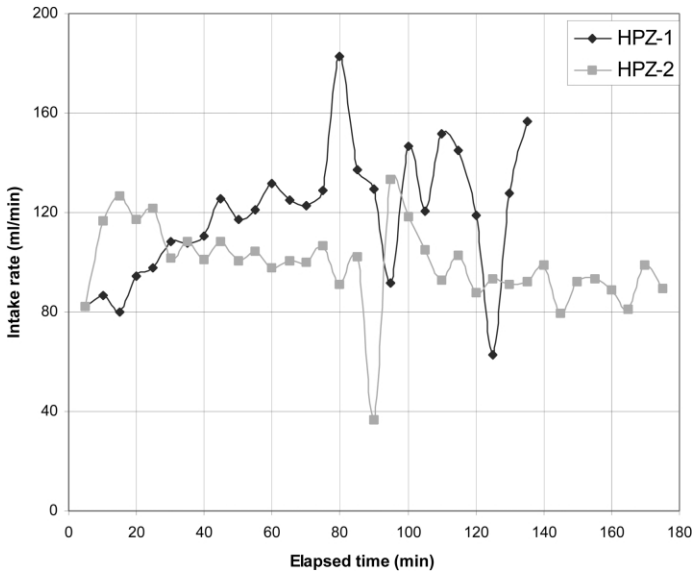

Fig. 6. Water intake rates observed in the HPZ.

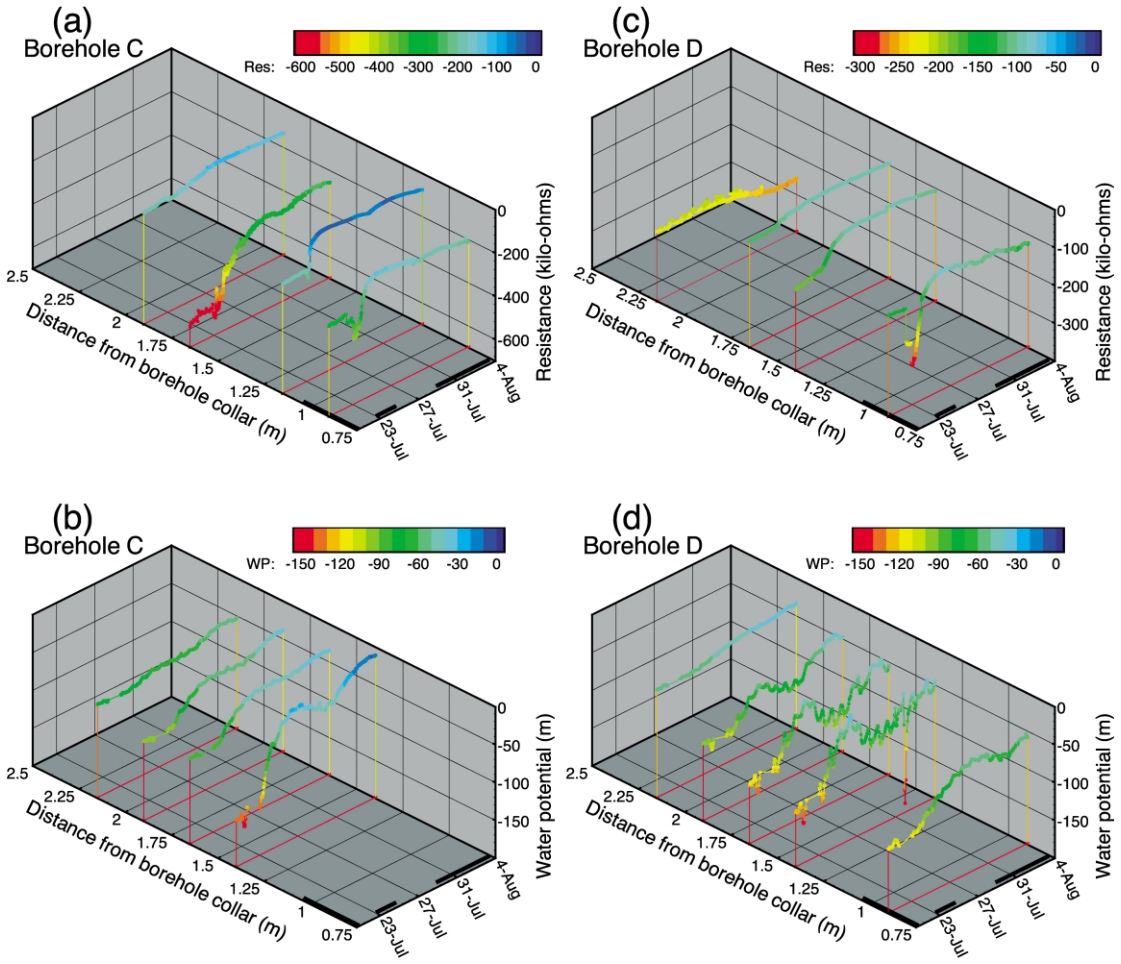

Fig. 7. Changes in electrical resistance and water potentials detected in boreholes 'C' and 'D' during liquid injection into the LPZ. Shaded zones indicate the location and duration of liquid-release events. Note resistance axis is inverted.

0.07 m in the injection zone. This constant-head was maintained for 4 h while the water level in the reservoir was continuously monitored. At the end of this constant-head period, water supply to the injection zone was discontinued, resulting in a falling-head boundary condition that lasted about one day. In total, 15 l of water were introduced into the LPZ during the constant-head and falling-head periods.

The final release into the LPZ was initiated on 7/29/98, when water was introduced into the formation under a constant-head maintained for 43 h, after which ponded water in the injection zone continued to percolate into the formation under a falling-head for four days. During the test, 1.0 l of water was released under the constant-head boundary and 1.2 l were released under the falling-head.

In summary, 9.2 l of water were released to the formation under a combination of constant- and falling-head boundary conditions in the LPZ.

Water was injected into the HPZ during two groups of tests over a period of two weeks (Table 2). The first group of four tests was conducted during 8/4–6/98; the second group was conducted during 8/25–27/98. The first two tests in the first group were constant-head tests that served to establish the intake rates at which the injection zone could release water to the formation. The first constant-head test had an average rate of ~119 ml/min, the second rate was ~98 ml/min.

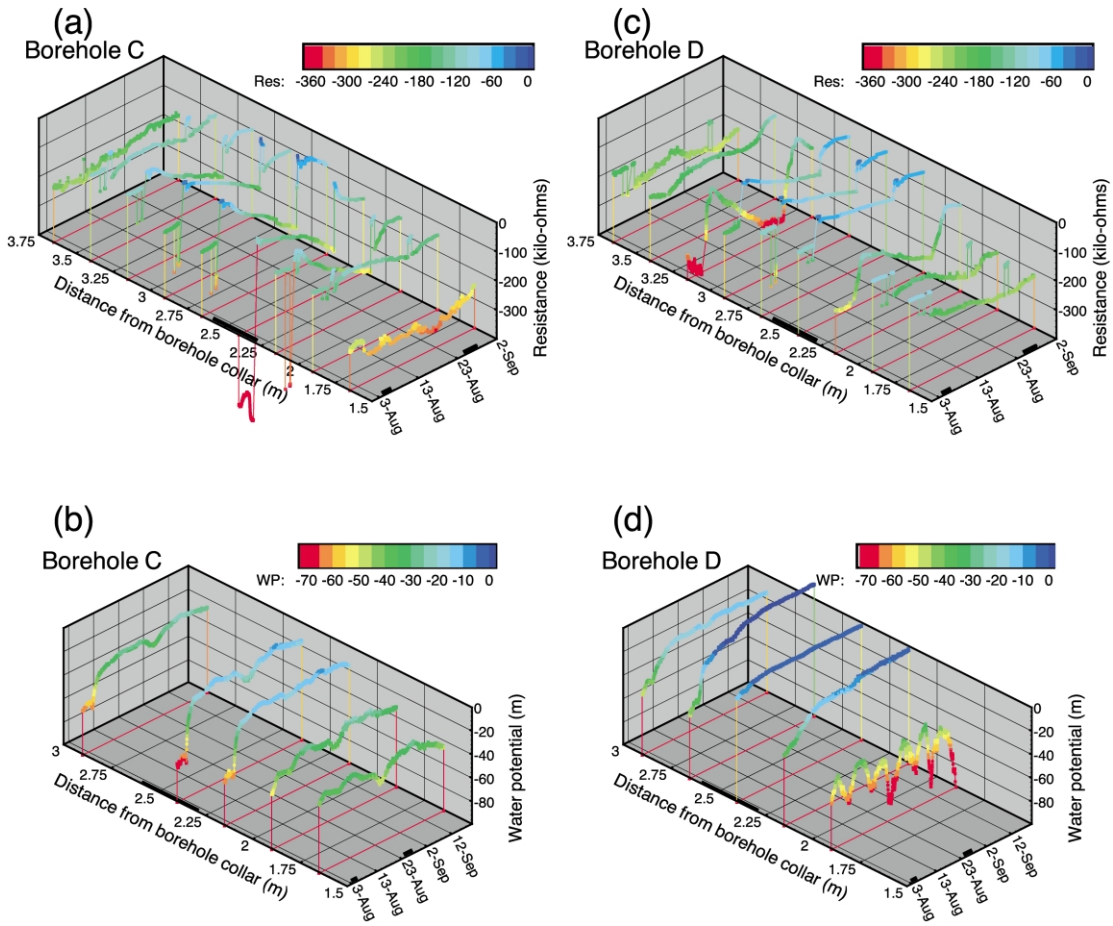

Fig. 8. Changes in electrical resistance and water potentials detected in boreholes 'C' and 'D' during liquid injection into the HPZ. Shaded zones indicate the location and duration of liquid-release events. Note resistance axis is inverted.

During the third test, conducted the next day, water was injected at approximately half the intake rates observed with the constant-head system (i.e. ~53 ml/min). During the fourth test on 8/6/98, water was injected at a constant rate of ~5 ml/min over 12 h. During the second group of tests (over a period of four days starting on 8/25/98), the injection rate was sequentially reduced from 69, 38, 29, and finally to 14 ml/min.

3. Observations

Water released in the injection borehole flowed through the fractured rock and, in the case of the HPZ, some of the water seeped into the slot located 1.6 m below. Liquid-release rates in the injection zone were measured, saturation and water potential changes were observed along monitoring boreholes, and water seeping into the slot was collected.

3.1. Liquid-release rates

Measurements of liquid-intake rates in the LPZ of the test bed exhibited a response similar to that observed for soils (Horton, 1940) and other fractured rock experiments (Kilbury et al., 1986; Faybishenko et al., 2000). The initially high-rates asymptotically approached low steady state values of ~0.35 ml/min (Fig. 5a). Near continuity was observed in the

Table 3
Summary of liquid injection test results in the high-permeability zone (volumes in l; time in h:min; injection rates in ml/min)

Test #	Injection rate	Duration of injection	Volume injected	Volume recovered	Travel time of first drop	Volume of water in formation		Water retained in formation (%)
						At first drop	At end of injection	
HPZ-1	119	2:17	16.28	11.61	0:05	0.41	4.67	29
HPZ-2	98	2:56	17.44	12.17	0:03	0.17	5.27	30
HPZ-3	53	5:25	17.45	11.14	0:03	0.14	6.31	36
HPZ-4	5	11:54	3.39	0.36	5:00	1.51	3.03	89
HPZ-5	69	4:26	18.37	11.47	0:03	0.14	6.90	38
HPZ-6	38	8:00	18.44	14.73	0:07	0.26	3.71	20
HPZ-7	29	10:36	18.23	13.21	0:07	0.20	5.02	28
HPZ-8	14	11:19	9.38	4.56	1:08	0.90	4.82	51

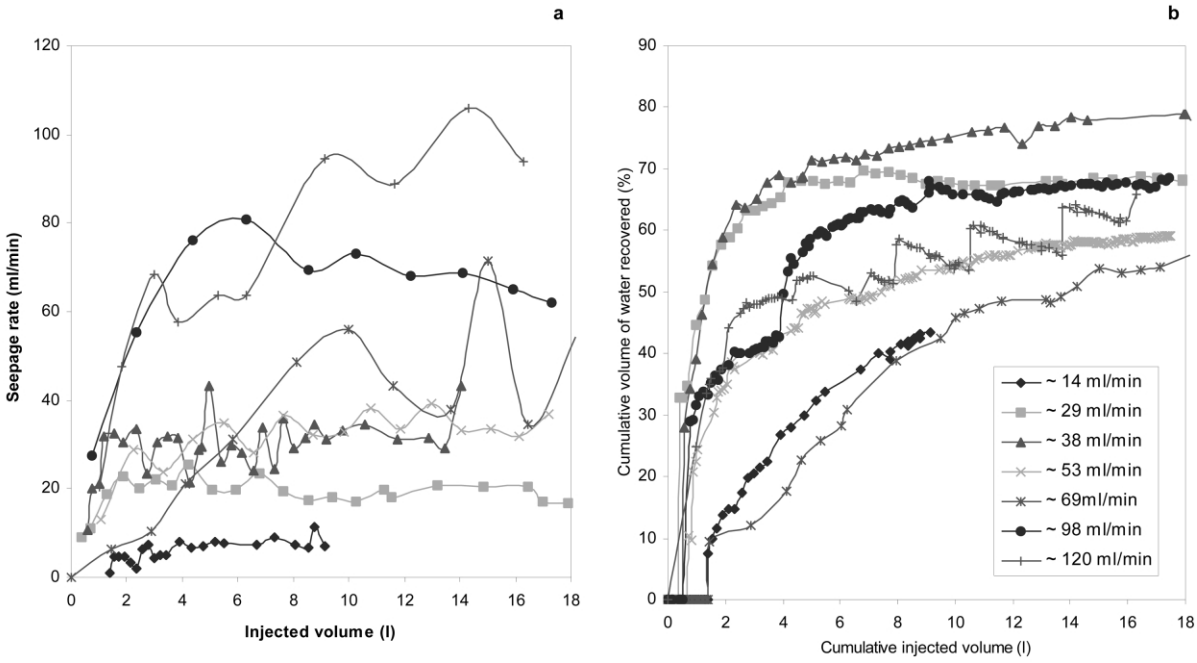

Fig. 9. Seepage into slot: (a) seepage rates for various HPZ tests and (b) cumulative percentage of injected water recovered.

decreasing liquid-intake rates even with a five-days gap between liquid-releases into the formation (Fig. 5b).

For the first two constant-head tests conducted in the HPZ, the rates of liquid-intake varied significantly during and between tests (Fig. 6). In the first test, the liquid-intake rate climbed for the first 60 min and then remained steady for the next 15 min before briefly increasing sharply. For the remainder of the test, the rate fluctuated between 70 and 160 ml/min. In the second test, the liquid-intake rate rapidly increased for the first 15 min. The rate then slowly decreased and leveled off near ~100 ml/min. Ninety minutes into the test, the liquid-intake rate briefly fell to 35 ml/min, sharply increased to 130 ml/min, and then slowly dropped down to a quasi-steady rate of 90 ml/min in the next 80 min.

3.2. Formation wetting and drying

During the LPZ tests, changes in saturation were detected by both the ERPs (Fig. 7a and c) and psychrometers (Fig. 7b and d) in the monitoring boreholes C and D in response to liquid-releases located 0.75–1.05 m from the borehole collar of injection borehole A. No response was detected in borehole B. In both boreholes C and D, large changes in saturation were detected by either or both ERPs and psychrometers located between 0.9 and 1.9 m from the collar. At a distance of 2.15 m from the borehole collar, the changes were much smaller.

During the HPZ tests, changes in saturation were detected by both the ERPs (Fig. 8a and c) and psychrometers (Fig. 8b and d) in the monitoring boreholes from liquid-releases located 2.30–2.60 m from the collar of injection borehole A. The zones between 2.15 and 2.40 m in borehole C and between 2.15 and 2.65 m in borehole D showed the largest changes during testing.

In both boreholes, the ERP and psychrometer data suggest that after the first batch of water releases (i.e. 8/4–6/98), saturation significantly increased. At most borehole D sensor locations, this increase persisted until the start of the second period of injection (8/25–28/98), at which time more water was retained by the formation, resulting in further increases in saturation. In contrast, in borehole C, psychrometer and especially ERP data show that significant drying occurred in between the two series of tests.

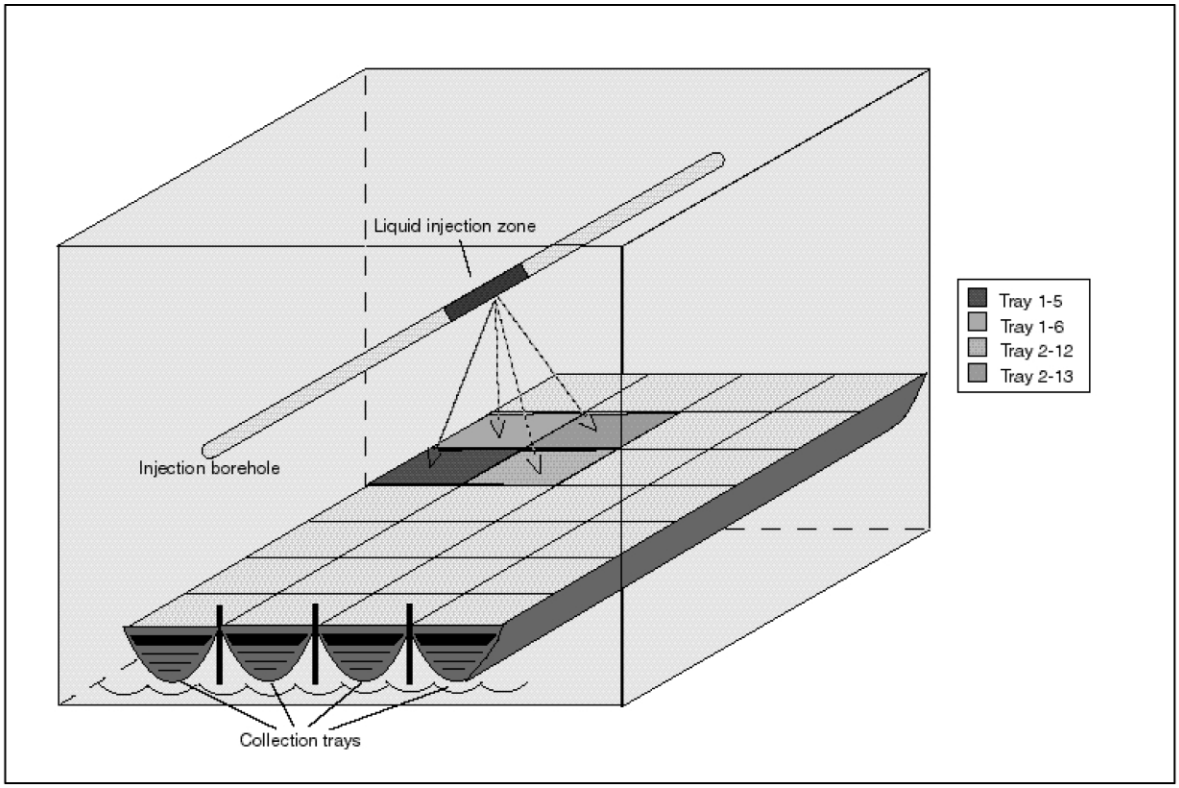
Liquid injection zone
Injection borehole
Collection trays
Tray 1-5
Tray 1-6
Tray 2-12
Tray 2-13


PERCENTAGE OF LIQUID RECOVERED FROM SLOT TRAYS AT DIFFERENT INJECTION RATES
% of injected fluid recovered
Injection rate (ml/min)
0
20
40
60
80
100
120
Tray 1-5
Tray 1-6
Tray 2-12
Tray 2-13
Tray-Total

3.3. Seepage into the slot

Seepage into the slot was observed during all eight tests in the HPZ (test results are summarized in Table 3). The eight tests were conducted in two groups (see Table 2). During the first test in the first group (HPZ-1), water was first observed on the slot ceiling within 5 min, after 0.41 l of water was released under constant-head conditions. In the second and third tests, water appeared in the slot within 3 min, after 0.17 and 0.14 l, respectively, had been released. In the fourth test, water appeared in the slot after 5 h, with 1.50 l of water injected at a rate of 5 ml/min.

In the second group of tests, travel time for the first drop of water was 3 min, after 0.14 l was injected at a rate of ~69 ml/min (HPZ-5). In the two subsequent tests, the arrival time of the wetting-front was 7 min, after 0.26 and 0.20 l of water were injected at a rate of 38 and 29 ml/min, respectively. In the final test, water first appeared in the slot after 68 min, with 0.90 l injected into the formation at a rate of 14 ml/min.

Large variability was observed in the slot seepage rate during and between HPZ tests (Fig. 9a). Intermittent seepage behavior was observed during all the tests, in which the rhythmical response that developed early in the test persisted for the duration of the test. Similar unsteady seepage has been observed in laboratory experiments of fracture flow (e.g. Persoff and Pruess, 1995; Glass et al., 1995; Kneafsey and Pruess, 1998; Su et al., 1999). Using parallel-plate experiments, Su et al. (1999) demonstrated that such cyclic behavior occurred when water flowed through a sequence of small to large to small aperture flow paths, which resulted in strong capillary forces periodically snapping threads of liquid. Another possible cause of seepage intermittency is changes to the fracture network itself, including mechanical instability of the fracture coatings and filling materials as well as mineral or salt dissolution and precipitation (Weisbrod et al., 2000; Dahan et al., 2000).

Because of the variability in slot seepage rate, it is more convenient to compare the cumulative percentage of injected water that is recovered at the slot for the various HPZ tests (Fig. 9b). This measure is a normalized integral of slot seepage rate. For a constant seepage rate, the cumulative percentage recovered would increase rapidly after the first drop of water arrived. The rate of increase would then smoothly decline until the cumulative percentage recovered reached a constant value (the ratio of the seepage rate to the injection rate). This would occur when the total volume injected became large compared to the volume that had been injected when seepage into the slot began. For the most part, the cumulative percentages recovered shown in Fig. 9b display these characteristics. An exception is test HPZ-1 (injection at 119 ml/min), in which the saw tooth cumulative percentage recovered suggests a strongly pulsed seepage rate. For most of the tests, the cumulative percentage recovered approached relatively constant values after approximately 10 l of water had been injected. However, tests HPZ-4 and HPZ-8 were not run long enough to show a constant cumulative percentage recovered.

Fig. 10 shows the distribution of seepage among the collection trays in the slot. During each test, water appeared on the slot ceiling at one single point below the injection zone. The spot could be identified by a rust spot approximately 0.05 m in diameter that developed on the I-beam separating trays 1–6 and 2–13. Seepage water was collected from four trays located around this localized point of entry. During these tests, water seeping into the slot was largely concentrated in a single tray, with the three other trays collecting significantly smaller amounts of water. Slight increases at higher injection rates were noticeable in some of the secondary trays. The remaining 24 trays stayed dry during all the liquid-release tests. A horizontal borehole located at the same height as the slot and approximately 1.0 m to its left was instrumented with ERPs and psychrometers that were monitored throughout the tests (Fig. 1). None of the instruments showed evidence of water flow to the left of the slot, supporting the hypothesis that none of the injected water bypassed the slot.

In all the tests during which there was seepage,

Fig. 10. Seepage into collection trays in the slot: (a) tray configuration and (b) final cumulative percentage of injected water recovered in different trays.

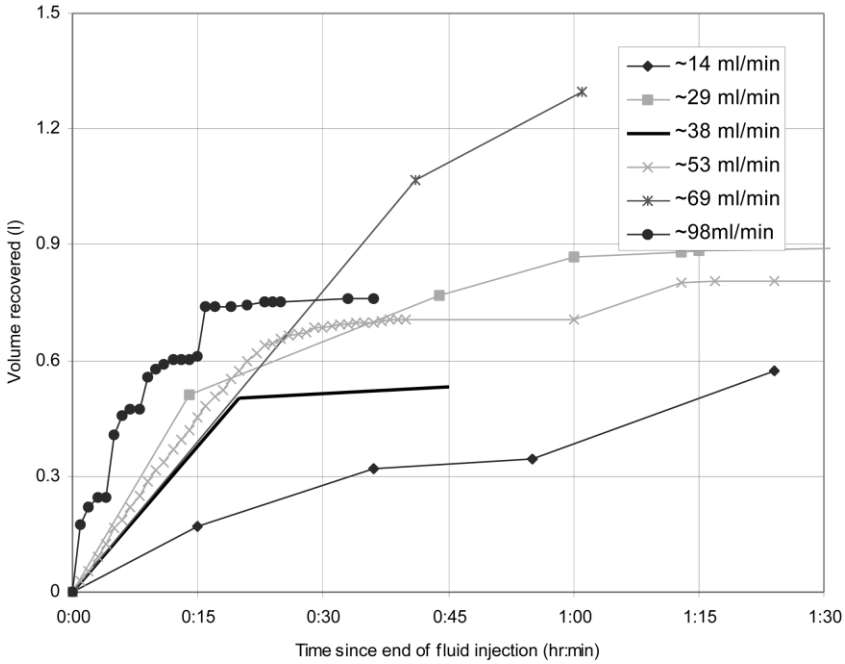

Fig. 11. Volume of water recovered in the slot after liquid injection to the HPZ was stopped.

0.5–1.3 l of water entered the slot after water supply to the formation was switched off (Fig. 11). Most of this water was collected within 1 h, with recovery rates being largest immediately after the test. The constant-head test with ~98 ml/min release rate (HPZ-2) had a 'stepped' nature to the post-injection recovery. During the first 15 min, the 0.8 l of collected water appeared in four bursts, each containing 0.1–0.3 l of water. Changes of similar magnitudes were observed in the tests with injection rates of ~53 (HPZ-3) and ~14 ml/min (HPZ-8).

3.4. Tracer recovery

While none of the tracers introduced in LPZ was recovered, all tracers injected in the HPZ were detected in the water samples collected in the slot (Hu et al., 2001). Typically, tracers introduced in one test were rapidly flushed out of the system during the subsequent test (Fig. 12). The pattern of recovered concentrations of tracers suggests that plug flow was the dominant process by which 'new' water replaced 'old' water from the previous test.

4. Discussion

The liquid-release tests conducted in two zones only 1 m apart demonstrate significant variability in hydrologic response. The formation response to liquid-releases in the LPZ suggests a conceptual flow model consisting of a strongly heterogeneous fracture network in which the high-permeability fractures are not extensive or are poorly connected. The closed-end features tend to wet up early and remain saturated throughout the remainder of the test. The key features of the data supporting this model are: (1) the large, continuous decrease in formation intake rate for sequential tests separated by a dry period (high-permeability closed-end fractures fill up first and thereafter do not participate; smaller interconnected fractures control the long-time injection rate); (2) the gradual responses of the monitoring borehole sensors, some of which monotonically reach steady state and some of which show a dynamic response corresponding to closed-end and inter-connected fractures, respectively; (3) the lack of through-flow to the slot (no long, inter-connected vertical fractures). In contrast to the continuously decreasing intake rate

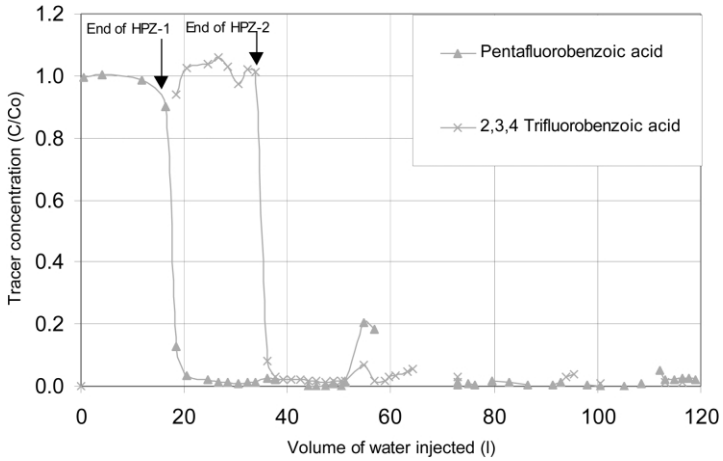

Fig. 12. Tracer concentrations in seepage water following injection into the HPZ.

observed for the LPZ tests (Fig. 5), for a series of ponded infiltration tests conducted in fractured basalt (Faybishenko et al., 2000), each test started with a different high intake rate that subsequently decreased to a common value. There, the conceptual model considered the largest fractures to be well connected, and these fractures presumably had a chance to drain between infiltration tests.

In contrast to the liquid-release rates observed in the LPZ, the HPZ did not show large decreases in release rates as additional water was introduced into the formation (Fig. 6). Further, the rates fluctuated significantly during the entire duration of the liquid-releases at constant-head. Slot seepage rates also fluctuated strongly, whether liquid was injected under constant-head or constant-rate conditions. Flow between the injection interval and the underlying slot occurred quickly (1.6 m in 3–7 min) unless the injection rate was low. These features are consistent with a conceptual model dominated by high-conductivity, well-connected fracture flow paths. Furthermore, the localized water arrival at the slot suggests that flow predominantly occurred in a few preferential, channelized pathways, the 'fast flow paths' commonly associated with partially-saturated high-conductivity fractured rock (Pruess, 1999; Pruess et al., 1999; Su et al., 1999). Strongly fluctuating, spatially localized flow was also observed during field experiments conducted in basalt (Podgorney et al., 2000) and chalk (Dahan et al., 2000) where flow appeared to be localized in a prominent fracture.

Generally, the monitoring borehole ERP and psychrometer responses were more abrupt for the HPZ tests than for the LPZ tests, consistent with the concept of a higher-conductivity, better-connected fracture network. Unfortunately, the ERP data, which shows sudden jumps suggestive of the kind of fluctuating, localized flow expected in fractured rock, also shows sudden jumps in resistivity that do not seem entirely plausible based on physical principles (e.g. simultaneous resistivity jumps at multiple sensors), making definitive inferences problematic. The relative locations of the HPZ injection interval and the slot location where breakthrough was centered (tray 1–6) suggest that borehole C should have shown larger responses than borehole D (compare Figs. 1b and 10a). In fact, Fig. 8 shows that although some of the largest saturation increases were noted in borehole D, the more dynamic responses were observed in borehole C, consistent with the notion of a through-going flow path there.

Volume estimates for water present in the vertical fast flow paths can be made from both early and late stages of the tests in the HPZ. Tests with relatively high injection rates (i.e. 29–100 ml/min) are particularly useful for estimating the volume of water occupying fast flow paths from early-stage data, because transit time between the injection interval and the slot is minimal, lessening the potential masking effects of lateral spreading, fracture/matrix interactions, and other capillary-driven flow. Here, the vertical flow-path volume between the injection

zone and slot ceiling can be assumed to be the volume of water injected during each test before the arrival time of the first drop into the slot (Table 3). For the first test, when the test bed was undisturbed, this approach will over-estimate fast-path volume because it includes an additional loss to closed-ended fractures. An estimate of this loss is provided by the difference between the volume of water taken by the formation early in the first and second tests (i.e. $0.41 - 0.17 = 0.24$ l). Observations from the later tests suggest that the fracture-flow-path volume during the early stages of each test ranged between 0.14 and 0.26 l.

A second estimate of the volume of vertical flow paths can be extracted from the post-injection seepage data (Fig. 11) where the amount of water collected varied between 0.5 and 1.3 l for water released at rates between 14 and 69 ml/min (since post-injection seepage for the constant-head injections included a finite volume of water from storage in the injection zone ($\sim$1.2 l), the first two tests have been excluded in these estimates). While these volumes are significantly greater than estimates from the prior analysis of early transient data, they may underestimate vertical-flow-path volumes in situations where water is held up in fractures by capillary forces.

Our data indicate that between 60 and 80% of the injected water was recovered by the end of each of the high-rate injection tests in the HPZ. With the test bed geometry and our conceptual model for flow arising from both the LPZ and HPZ tests, we are reasonably confident that the remaining 20–40% remained in the fractured rock formation, either held up by capillarity on the walls of the fast flow paths, trapped in high-permeability closed-end fractures, moving slowly through low-permeability connected fractures, or imbibed into the matrix. Numerical modeling of the LPZ and HPZ tests based on this conceptual flow model and an investigation of possible fast flow path geometries that would be consistent with the data are presented in a companion paper (Doughty et al., 2001).

5. Conclusions

The main objective of this paper is to present fracture flow data collected during a liquid-release test conducted in a slotted test bed located in a highly fractured, densely welded tuff at Yucca Mountain. Because of the slot, it was possible to quantify flow both into and out of the test bed and better understand the nature of the flow. Test results revealed a wide range of fracture flow behavior and provided insight towards the conceptualization of flow through unsaturated, fractured rock formations in which both fracture flow and fracture/matrix interactions play important roles. In particular, declining water intake rates and diffuse migration patterns observed during the LPZ tests suggest that the largest fractures do not always form a connected path. In contrast, the rapid water arrivals, fluctuating injection and seepage rates, and incomplete water recovery characteristic of the HPZ tests indicate that one or more large fractures form a continuous, variable-aperture pathway, while the smaller, less well-connected fracture network continues to play an important role.

Results from field tests indicate that the techniques developed to investigate flow in fractured, welded tuffs are effective for in situ characterization of certain fundamental flow parameters (such as travel times, percolation paths, and seepage rates, etc.). Innovations that may prove generally useful for field investigations in unsaturated fractured rock include techniques to drill and stabilize a slot beneath the test bed, automatic controllers for liquid-release under constant-head or flow rate conditions, BSTs including psychrometers and ERPs to monitor moisture changes, and compartmentalized collection trays enabling spatial resolution of seepage and tracer breakthrough. Improvements in automation are being developed to overcome the constraints on test design arising from limited access to the test bed that were encountered in the field studies.

Acknowledgements

This work was supported by the Director, Office of Civilian Radioactive Waste Management, through Memorandum Purchase Order EA9013MC5X between TRW Environmental Safety Systems Inc. and the Ernest

Orlando Lawrence Berkeley National Laboratory for the Yucca Mountain Site Characterization Project through US Department of Energy Contract No. DE-AC03-76SF00098. Thanks are due to Robert Conroy, Paul Cook, John Dinsmoor, Jose Gonzales, Manuel Gonzales, Margaret Guell, Qinhong Hu, Lee Jacobs, Alan Mitchell, Gene Pokorny, Jan Stepak, Robert Terberg, Tetsu Tokunaga, and Robert Trautz for assistance in developing various aspects of the field experiments. Reviews of the manuscript by Peter Persoff, Tim Kneafsey and Dan Hawkes are gratefully acknowledged.

References

Cook, P., 2000. In situ pneumatic testing at Yucca Mountain. Int. J. Rock Mech. Mining Sci. 37, 357–367.

Dahan, O., Nativ, R., Adar, E., Berkowitz, B., 1998. Measurement system to determine water flux and solute transport through fractures in the unsaturated zone. Ground Water 36, 444–449.

Dahan, O., Nativ, R., Adar, E.M., Berkowitz, B., Ronen, Z., 1999. Field observation of flow in a fracture intersecting unsaturated chalk. Water Resour. Res. 35, 3315–3326.

Dahan, O., Nativ, R., Adar, E.M., Berkowitz, B., Weisbrod, N., 2000. On fracture structure and preferential flow in unsaturated chalk. Ground Water 38, 444–451.

Davidson, G.R., Bassett, R.L., Hardin, E.L., Thompson, D.L., 1998. Geochemical evidence of preferential flow of water through fractures in unsaturated tuff, Apache Leap, Arizona. Appl. Geochem. 13, 185–195.

Doughty, C., Pruess, K., 1992. A similarity solution for two-phase water, air, and heat flow near a linear heat source in a porous medium. J. Geophys. Res. 97 (B2), 1821–1838.

Doughty, C., Salve, R., Wang, J.S.V., 2001. Liquid flow in fractured welded tuffs: II. Numerical modeling. J. Hydrol. 256 (1–2).

Fabryka-Martin, J.T., Dixon, P.R., Levy, S., Liu, B., Turin, H.J., Wolfsburg, A.V., 1996. Summary report of Chlorine-36 studies: systematic sampling for Chlorine-36 in the Exploratory Studies Facility, Los Alamos National Laboratory Milestone Report 3783AD, Los Alamos National Laboratory, Los Alamos, New Mexico.

Faybishenko, B., Doughty, C., Steiger, M., Long, J.C.S., Wood, T.R., Jacobsen, J.S., Lore, J., Zawislanski, P.T., 2000. Conceptual model of the geometry and physics of water flow a fractured basalt vadose zone. Water Resour. Res. 36, 3499–3520.

Glass, R.J., Nicholl, M.J., Tidwell, V.C., 1995. Challenging models for flow in unsaturated, fractured rock through exploration of small scale processes. Geophys. Res. Lett. 22, 1457–1460.

Haldeman, W.R., Chuang, Y., Rasmussen, T.C., Evans, D.D., 1991. Laboratory analysis of fluid flow and solute transport through a fracture embedded in porous tuff. Water Resour. Res. 27, 53–65.

Horton, R.E., 1940. An approach toward a physical interpretation of infiltration capacity. Soil Sci. Soc. Am. Proc. 4, 399–417.

Hu, Q., Salve, R., Stringfellow, W., Wang, J.S.Y., 2001. Field tracer transport tests in unsaturated fractured tuff. J. Contam. Hydrol. 51, 1–12.

Kilbury, R.K., Rasmussen, T.C., Evans, D.D., Warrick, A.W., 1986. Water and air intake of surface-exposed rock fractures in situ. Water Resour. Res. 22, 1431–1443.

Kneafsey, T., Pruess, K., 1998. Laboratory experiments on heat-driven two-phase flows in natural and artificial rock fractures. Water Resour. Res. 34, 1457–1460.

Lenormand, R., Zarcone, C., 1989. Capillary fingering: percolation and fractal dimension. Transp. Porous Media 4, 512–599.

Montazer, P., Wilson, W.E., 1984. Conceptual hydrologic model of low in the unsaturated zone, Yucca Mountain, Nevada. US Geol. Surv. Water Resour. Invest. Rep., 84–4355.

Nitao, J., Buscheck, T., 1991. Infiltration of a liquid front in an unsaturated, fractured porous medium. Water Resour. Res. 27, 2099–2112.

Paces, J.B., Newmark, L.A., Marshall, B.D., Whelan, J.F., Peterman, Z.E., 1996. Ages and origins of subsurface secondary minerals in the Exploratory Studies Facility, 1996 Milestone Report 3GQH450M, US Geological Survey, Denver, Colorado.

Persoff, P., Pruess, K., 1995. Two-phase flow visualization and relative permeability measurement in natural rough-walled rock fractures. Water Resour. Res. 31, 1175–1186.

Podgorney, R.K., Wood, T.R., Faybishenko, B., Stoops, T.M., 2000. Spatial and temporal instabilities in water flow through variably saturated fractured basalt on a one-meter field scale. In: Faybishenko, B., et al. (Eds.). Dynamics of Fluids in Fractured Rock. Geophysical Monograph Series, Vol. 122. American Geophysical Union.

Pruess, K., 1999. A mechanistic model for water seepage through thick unsaturated zones in fractured rocks of low matrix permeability. Water Resour. Res. 35 (4), 1039–1051.

Pruess, K., Tsang, Y.W., 1990. On two-phase relative permeability and capillary pressure of rough-walled rock fractures. Water Resour. Res. 26, 1915–1926.

Pruess, K., Wang, J.S.Y., 1987. Numerical modeling of isothermal and nonisothermal flow in unsaturated fractured rock: a review. In: Evans, D.D., Nicholson, T.J. (Eds.). Flow and Transport Through Unsaturated Rock. Geophysical Monograph Series, Vol. 42. AGU, Washington, DC, pp. 11–21.

Pruess, K., Faybishenko, B., Bodvarsson, G.S., 1999. Alternative concepts and approaches for modeling flow and transport in thick unsaturated zones of fractured rocks. J. Contam. Hydrol. 38 (1–3), 281–322.

Salve, R., Wang, J.S.Y., Tokunaga, T.K., 2000. A probe for monitoring wetting front migrations in rocks. Water Resour. Res. 36, 1359–1367.

Su, G., Geller, J.T., Pruess, K., Wen, F., 1999. Experimental studies of water seepage and intermittent flow in unsaturated, rough-walled fractures. Water Resour. Res. 35, 1019–1037.

Tokunaga, T.K., Wan, J., 1997. Water film flow along fracture surfaces of porous rock. Water Resour. Res. 33, 1287–1295.

Wang, J.S.Y., Narasimhan, T.N., 1985. Hydrologic mechanisms

governing fluid flow in a partially saturated, fractured, porous medium. Water Resour. Res. 21, 1861–1874.

Wang, J.S.Y., Trautz, R.C., Cook, P.J., Finsterle, S., James, A.L., Birkholzer, J., 1999. Field tests and model analyses of seepage into drift. J. Contam. Hydrol. 38, 323–347.

Weisbrod, N., Nativ, R., Adar, E.M., Ronen, D., Ben-Nun, A., 2000. Impact of coating and weathering on the properties of chalk fracture surfaces. J. Geophys. Res. B 105, 27853–27864.